Probabilistic UHF RFID tag pose estimation with multiple antennas and a multipath RF propagation model

Travis Deyle, Charles C. Kemp, and Matthew S. Reynolds

***Abstract*—We present a novel particle filter implementation for estimating the pose of tags in the environment with respect to an RFID-equipped robot. This particle filter combines signals from a specially designed RFID antenna system with odometry and an RFID signal propagation model. Our model includes antenna characteristics, direct-path RF propagation, and multi-path RF propagation. We first describe a novel 6-antenna RFID sensor system that provides the robot with a 360-degree view of the tags in its environment. We then present the results of real-world evaluation where RFID-inferred tag position is compared with ground truth data from a laser range-finder. In our experiments the system is shown to estimate the pose of UHF RFID tags in a real-world environment *without requiring a priori training or map-building*. The system exhibits 6.1deg mean bearing error and 0.69m mean range error over robot to tag distances of over 4m in an environment with significant multipath. The RFID system provides the ability to uniquely identify specific tagged locations and objects, and to discriminate among multiple tagged objects in the field at the same time, which are important capabilities that a laser range-finder does not provide. We expect that this new type of multiple-antenna RFID system, including particle filters that incorporate RF signal propagation models, will prove to be a valuable sensor for mobile robots operating in semi-structured environments where RFID tags are present.**

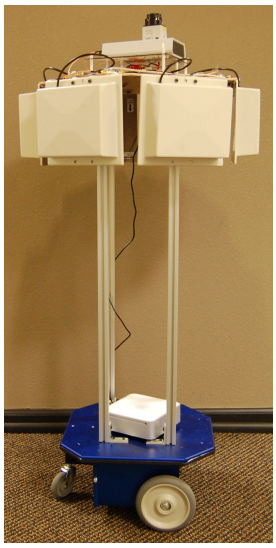

Fig. 1. Mobile robot with 6-antenna RFID sensor system

I. Introduction

Radio frequency identification (RFID) is an umbrella term for a variety of transponder systems, including active (battery-powered) and passive (battery-free) tags of widely varying complexity and capabilities. In this work we concentrate on simple, low-cost passive UHF RFID tags, often called "smart labels," based on the widely adopted EPC Global Generation 2 communication protocol [1]. Currently available passive UHF RFID tags are battery-free, with a read range exceeding 5 meters and data storage capacities ranging from 128 bits to over 1K-bit. They currently cost less than $0.10 USD in volume. To date, RFID tags have typically been used in a purely binary fasion, returning a tag ID if the tag can be read, or indicating that no tag was found. Prior work has shown how this binary tag sensing modality can be used to improve robot localization, mapping, navigation, and unique object detection. In this work we demonstrate that there is valuable information present in the tag's RF signal itself, beyond the tag ID. We present a novel enhancement to on-robot RFID sensing by leveraging robot mobility with a physical sensor model and a particle filter framework that provides relative tag pose (range and bearing to each tag from the robot's local frame of reference) in addition to tag presence or absence. This enhancement does not require *a priori* mapping, and does not require the collection of labor-intensive sensor histogram models.

In this work we leverage a unique element of passive tag behavior. Because passive RFID tags do not contain a battery, sufficient incident RF power must be available at the tag to allow its on-board circuitry to operate [2]. We take advantage of this tag power-up threshold to produce an estimate of the *forward path loss* between each of 6 robot-mounted reader antennas and each tag in the environment. The forward path loss is the difference between the amount of RF power transmitted by the reader and the amount of RF power actually reaching the tag, and is a function of reader antenna characteristics, tag antenna characteristics, and the range and bearing to the tag. We have developed a particle filter implementation for estimating each tag's range and bearing relative to a robot-mounted reader by employing the measured path loss from the robot to the tag in concert with direct-path and multi-path RF propagation models.

T. Deyle is with the Department of Electrical and Computer Engineering, Georgia Tech, Atlanta GA 30332

C. Kemp is with the Department of Biomedical Engineering, Georgia Tech, Atlanta GA 30332

M. Reynolds is with the Department of Electrical and Computer Engineering, Duke University, Durham NC 27708. e-mail: matt.reynolds@duke.edu

To make a path loss measurement to any tag regardless of its bearing with respect to the robot, we have developed an antenna array with 6 overlapping beams that achieves a 360-degree view of the robot's surroundings (see Fig. 2). This antenna array enables tag range and bearing estimation regardless of the robot's orientation at the time of measurement. We show that a factory measurement of antenna radiation pattern is sufficient to generate the physical model parameters employed in the particle filter which obviates the time-intensive histogram model generation employed in prior work (e.g. [3]). With this new approach, it is not necessary to build or have *a priori* knowledge of any histograms or maps for relative tag pose estimation.

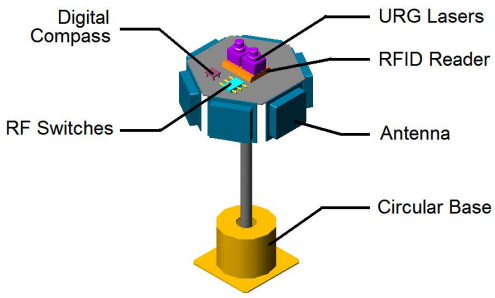

Fig. 2. Multiple antenna array shown with RFID reader and ground-truth capture equipment

Some potential RFID applications include enhanced navigation using reference waypoints, improved localization and mapping, robust object localization and interaction, mobile manipulation of tagged objects, and the development of robust human-robot interaction behaviors, such as people following. We expect that the contributions of this work in tag range and bearing estimation can be of value in all of these applications. The remainder of this paper will focus on implementation details and the results of several experiments to characterize RFID tag pose estimation accuracy compared with ground truth data obtained with a laser range finder.

II. Related Work

A wide variety of research has been conducted on the application of RFID technology to robotics. This includes RFID-enhanced interaction between robots and tagged people and objects, such as that described in [4], where tags facilitate person/object identification. There is also a great deal of prior work in RFID augmented indoor navigation [5], where tags are used as either a waypoint navigation and landmarking system [6], or more commonly as a component of a robot's localization and mapping system. Several recent works employ long-range passive UHF (902-928MHz) RFID, in addition to laser rangefinders and odometry, as sensor inputs to a probabilistic SLAM algorithm, for example [3]. In these prior results, the RFID system merely reports the tag IDs of visible RFID tags, or indicates that no tag is found. Our new work explicitly takes advantage of RF signal information in the probabilistic framework, while in the prior work any information present in the RF signal itself is discarded before the tag IDs reach the robot's navigation system.

An alternative RFID-enhanced navigation approach uses short-range ($\approx$1m) magnetically coupled passive RFID tags [7] to detect when robots pass above tagged waypoints. Again, however, a binary indication of tag presence or absence is all that is reported by the RFID system. Recent work in *active* (battery-powered) tagging [8] demonstrates navigation to a relatively expensive, battery powered target tag in a cluttered environment. In the latter work, a mechanically rotating reader antenna with a deep null in its radiation pattern is used to find bearings from the reader to the active tag. In this work, the RF signal strength is incorporated into the robot's navigation system, but [8] relies on expensive battery-powered tags and requires a rotating antenna on the robot, which is mechanically complex and limits update rate to the achievable mechanical rotation rate for the antenna motor. Other complex or expensive tag-centric antenna design techniques have also been explored to find range and bearing [9].

In the prior work where passive UHF RFID is used, e.g. [3], the tag reader has provided identity information only; that is, the tag is either read or not read (tag ID present or absent), and the result of the read attempt is taken as a binary variable. In the approach of [3], a tag read/not read histogram approach is inherent to the posterior update of robot's belief state. In that work, a model was built in a training configuration using a 12,822 measurement histogram created by mounting the tag on a box and counting the number of successful tag reads for a wide variety of different tag ranges and bearings with respect to the reader. A greatly simplified discrete likelihood detection region model (Fig. 4 in [3]) was then used to estimate the likely locations of the tags given an assumed map of the environment derived from a laser scanner and a FastSLAM implementation. This approach is adequate for line-of-sight applications where multipath propagation is not prevalent, and where many tags are simultaneously visible to the reader, but the histogram approach requires an extremely large number ($>$10,000 in some cases) of binary measurements and substantial training time to result in a useful tag position estimate because of the typically large read zone (10m^2 to 25m^2) available in front of each antenna.

In contrast, in this work we look beyond the binary "presence/absence" indication by leveraging an important continuous-valued statistic of the RF signal itself. We employ the tag's power-up threshold (the incident RF power level at which the tag receives enough power to operate) to provide a continuous-valued measurement of the *forward path loss* from each of 6 robot-mounted antennas to each tag in the environment. Because each of the antennas has a beam width of over 60 degrees, the 6 antenna array is capable of observing tags at any bearing with respect to the robot without requiring any mechanical motion of the antennas or the robot. We show that the path loss measurements, when coupled with a physical model of RF propagation, can be employed as a

continuous-valued statistic in a particle filter implementation that eliminates the requirement to collect histogram training data. Furthermore, the particle-filter's maximum-likelihood tag pose estimate is relative to the robot's local frame of reference, and thus does not require a pre-built map to find tag range and bearing, though if a SLAM implementation is desired the forward path loss statistic is also straightforward to use in a probabilistic SLAM implementation such as the one presented in [3].

III. Multiple-antenna RFID reader apparatus

In order to evaluate the performance, precision, and accuracy of the RFID sensor and particle filter implementation, we first conducted a series of tests with a static test rig as shown schematically in Figure 2. We employed the following components in these tests:

- **RFID Reader:** ThingMagic Mercury 4e UHF RFID reader with two antenna ports.
- **RF Switches:** Two Skyworks AS195-306 RF switches controlled via USB and connected to multiplex the RFID reader's two antenna ports to 6 antennas.
- **Antennas:** Six MaxRad MP8906PTNF patch antennas (70-degree horizontal, 50-degree vertical beam angle).
- **Digital Compass:** Ocean Server OS5000 tilt-compensated digital compass.
- **Laser Scanners:** Two Hokuyo URG-04LX laser rangefinders ($\approx$ 4m range) for obstacle/wall detection.
- **Laser Target:** A cardboard cylinder was used as a laser target for a SICK LMS291 laser rangefinder providing ground truth.

After testing, the multiple antenna RFID apparatus was mounted on the mobile robot base shown in Figure 1 for mobile operation.

IV. Integrating RF propagation models into the particle filter

We employ a particle filter framework based on the low variance resampling implementation from [10]. We wish to find the posterior $p(x_t|z_{1:t}, u_{1:t}, x_{1:t})$, where x is the state variable representing tag pose relative to the robot, $z_{1:t}$ are RFID measurements from all previous time steps, and $u_{1:t}$ are a set of controls (odometry updates) over all time steps. We apply Bayes' rule with a first order Markov model to yield the recursive expression

$$p(x_t|z_{1:t}, u_{1:t}, x_{1:t}) = \eta \cdot p(z_t|x_t) \cdot p(x_t|u_t, x_{t-1}) \quad (1)$$

In this formulation, $p(x_t|u_t, x_{t-1})$ represents a motion model or control (odometry for our implementation, as discussed in [10]), η is a normalization factor, and $p(z_t|x_t)$ is the sensor model we desire to explore. In this expression, $p(z_t|x_t)$ represents the probability distribution of the sensor measurement (i.e. reading/not reading a tag) given a current state including the range and bearing to the particle under consideration.

In this work we present a new model for thinking about the distribution, $p(z_t|x_t)$, based on a physical model of RF signal propagation rather than an empirically-generated histogram model as was used in [3], in order to obviate extensive empirical training. Instead, we use an RF propagation model including the RFID reader's transmission power and antenna characteristics to predict the far-field read range using the Friis free space RF propagation model [11] with extensions to handle multipath propagation indoors.

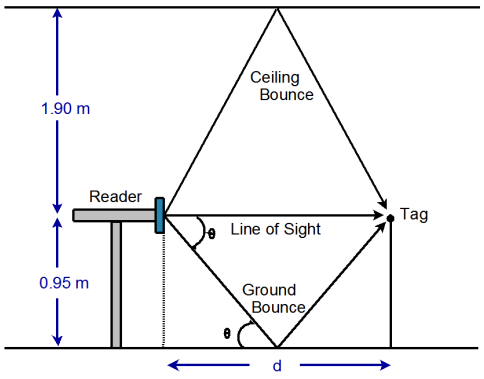

Fig. 3. RF propagation indoors including including direct path, ground bounce multipath, and ceiling bounce multipath

A. Tag power-up and the forward link limit

In order to make inferences about the likelihood of a tag being read in a certain state configuration x_t, we must first understand what factors influence tag readability. This is relatively straightforward in the passive UHF RFID case as one factor is dominant; since tags do not have batteries they must derive their operating power from the incoming RF signal transmitted by the reader. If insufficient RF power is incident on the tag, the tag will not power up and will be completely inert. Thus the potential readability of a particular tag given a state configuration x_t and an RF signal path associated with x_t is governed by the 'forward link limited' condition. The forward link limit occurs when the incident power at the tag P_{tag}^{inc} just equals the power up threshold of the tag P_{tag}^{th}, i.e. the tag is just operating, but any decrease in incident power will result in the tag becoming inoperative. We have determined that the RFID reader's receiver has an excess of sensitivity, so as long as the tag is powered up, the reader will receive the tag signal with probability arbitrarily close to unity. In this condition we call the RFID system 'forward link limited' because the delivery of power from the reader to the tag is the primary criterion for successfully reading the tag. We use this threshold requirement to define the measurement model as follows:

$$p(z_{t_i} = \text{Present}|x_t) = \begin{cases} 1.0 & \text{if } P_{tag}^{inc} \geq P_{tag}^{th} \\ 0.6 & \text{otherwise} \end{cases}$$

$$p(z_{t_i} = \text{Absent}|x_t) = \begin{cases} 1.0 & \text{if } P_{tag}^{inc} < P_{tag}^{th} \\ 0.6 & \text{otherwise} \end{cases}$$

A number of read attempts are performed per measurement update, as our algorithm sweeps across multiple power levels and across all 6 antennas, to yield a probability distribution

$$p(z_t|x_t) = \prod_{\substack{\text{powers} \\ \text{antennas}}} p(z_{t_i}|x_t) \tag{2}$$

The decision region is fundamentally defined by the relationship between P_{tag}^{inc} and P_{tag}^{th}. The latter is specified by the tag manufacturer, while the former can be estimated using the well-known Friis free space RF propagation model [11]. The expressions above define a spatial probability distribution that is effectively sampled by particles. Figure 4 shows the two distinct distributions employed in the tag present and tag absent cases. The numerical weight values were determined experimentally to provide good convergence and sufficient generalization, but are in similar proportion to the weights found in the histogram methods of [3].

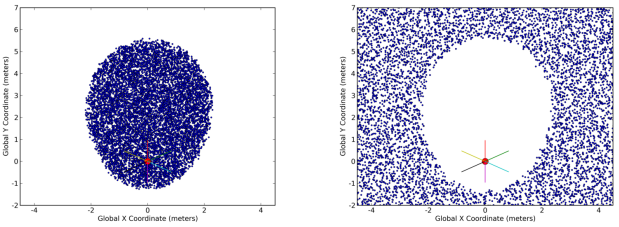

Fig. 4. Update weighting. *Left:* When a tag is read, any particle inside the Friis model read-range estimate is weighted by 1.0, any outside by 0.6. *Right:* When a tag is **not** read, any particle inside the Friis model read-range estimate is weighted by 0.6, any outside by 1.0.

B. The Friis free space RF propagation model with multipath extensions

To find the power incident on the tag, we traverse the signal path (for each path, including line-of-sight and all reflection paths) multiplicatively accounting for each component's gain/loss. To determine the incident power at the tag due to a single path, we start with the reader's transmitted power P_{rdr}, account for the cable loss CL, multiply by the gain of reader antenna $G_{rdr}(\theta)$ for each path, include the free-space loss due to the spreading of the beam over that path (called path loss or PL), and finally, account for the tag antenna's gain G_{tag} to arrive at the incident power on the tag integrated circuit. We make explicit the possibility of multipath by summation of incident power over all paths:

$$P_{tag}^{inc} = \sum_{\text{all paths}} P_{rdr} \cdot CL \cdot G_{rdr}(\theta) \cdot PL \cdot G_{tag} \tag{3}$$

In most situations, P_{rdr}, CL, and G_{tag} are constants for all paths, which reduces Eq. 3 to

$$P_{tag}^{inc} = P_{rdr} \cdot CL \cdot G_{tag} \cdot \left[\sum_{\text{all paths}} G_{rdr}(\theta) \cdot PL \right] \tag{4}$$

$G_{rdr}(\theta)$ is the antenna radiation pattern and is readily available from the antenna manufacturer. We estimate path loss with the Friis model, which is derived from the spherical geometry of the problem [11]:

$$PL = \left(\frac{3 \cdot 10^2}{4\pi \cdot d \cdot f} \right)^2 \tag{5}$$

where d is the distance (in meters) along the RF propagation path, and $f \approx 915$MHz is the operating frequency. Path distance d represents the distance between a particle under consideration and the robot. Fractional representations of all ratios must be employed in these calculations[1].

For a single (direct) path, substituting Eq. 5 into Eq. 4 yields the required incident power for a successful read as a function of distance to the tag. This relationship is illustrated in the measurement presented in Fig. 5, which shows good agreement between the Friis model and the measured incident power.

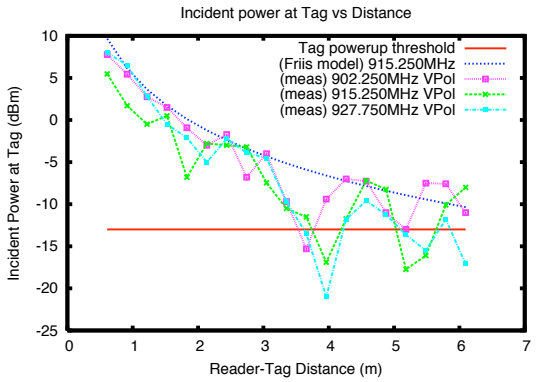

Fig. 5. Measured incident tag power versus distance from reader, as compared to the Friis model.

V. RF Propagation Model Parameters

In order to use the model quantitatively, we must know the model parameters P_{rdr}, $G_{rdr}(\theta)$, G_{tag}, CL, and P_{tag}^{th}. Values for some of these parameters can be taken directly from manufacturer's specifications. For example, RFID reader power Pwr_{rdr} can be set in software from 5dBm to 30dBm (3.1mW to 1W). Manufacturer's specifications provide P_{tag}^{th} as -13 dBm (50μW), and G_{tag} as 1 dBi.

A. Determining $G_{rdr}(\theta)$ and CL

It is common for antenna manufacturers to provide the antenna gain, $G_{rdr}(\theta)$, as a function of angle on the horizontal plane. The antenna gain for the MaxRad MP8906PTNF used in this paper is shown in Figure 6 as specified by the manufacturer, as observed experimentally with a series of actual tag reads in the laboratory, and as empirically fit with a second-order exponential.

To determine the cable and switch loss, CL, in the system, we can simply add together the losses along the cable and

[1]RF component parameters are frequently given in the log units of dB, given by $X_{dB} = 10 \cdot \log_{10} X$; values in dB must be converted to fractional ratios before use here.

switch path from the RFID reader to the antenna. In our system, the RF cables introduce a total of 1.5 dB in losses. The switches themselves also introduce an additional 1 dB of loss. Thus the total cable and switch loss CL = -2.5 dB.

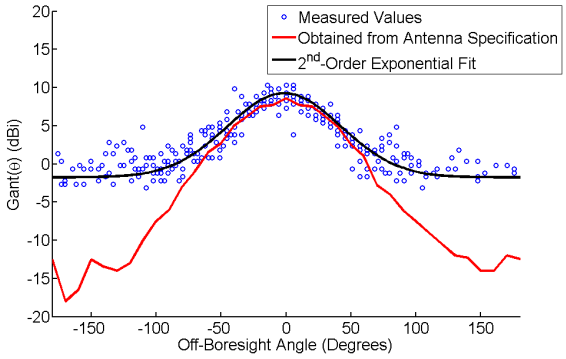

Fig. 6. $G_{rdr}(\theta)$ as specified in the MaxRad MP8906PTNF radiation pattern specification, plotted with a second-order exponential fit to the observed tag read profile.

VI. Experimental Results and Model Validation

Evaluation of the multiple antenna RFID system and the particle filter implementation was performed in a 10m×12m open room with ceiling height of ≈2.85m. The primary sources of multipath in this room are the ground and ceiling bounces from the reinforced concrete floor and ceiling. The robot base and its 6-antenna RFID system were configured to sample and capture in a data log file the observed tag readability with varying read power levels in between movement events of ≈ 20cm. Ground truth was obtained using a SICK LMS291 laser range-finder and a circular Hough transform to find the centroid of the circular cardboard laser targets surrounding the robot base and the tag. The orientation of the robot base was measured with the digital compass and cross-validated with manual angle measurements relative to room "north".

From these measurements, simulated odometric control updates, consisting of translation and rotation with Gaussian error profiles, were projected into the robot's local frame for input to the particle filter. The particle filter's initial state consisted of 1000 particles uniformly spaced over a $20m \times 20m$ grid, centered about the robot. Control updates and RFID read events from all 6 antennas over 9 read power levels were extracted from the logged dataset for each 20 cm of robot movement. Measurement update rate is dominated by tag read times of 1-3ms and antenna switching times of 6ms, yielding 6-antenna update times of 50-100ms. The results of this evaluation are shown graphically in Figure 7 and numerically in Table I, where μ = mean, σ = standard deviation and

$$d_{error} = |d_{actual} - d_{estimated}|$$

$$d_{relative} = |d_{error} \div d_{actual}|$$

$$\theta_{error} = |\theta_{actual} - \theta_{estimated}|$$

While we employed 1000 particles in this experiment to better quantify the variance, the particle filter is capable of converging on an equally-accurate mean estimate with fewer than 40 particles.

Range	Error Measures	Line-Of-Sight Only	With Ground & Ceiling Bounce
All d_{actual}	d_{error}	μ=0.71m σ=0.45m	μ=0.69m σ=0.42m
	$d_{relative}$	μ=16.2% σ=6.8%	μ=15.9% σ=6.6%
	θ_{error}	μ=6.11^o σ=4.19^o	μ=6.11^o σ=4.19^o
$d_{actual} \leq$ 4 m	d_{error}	μ=0.40m σ=0.20m	μ=0.41m σ=0.21m
	$d_{relative}$	μ=13.3% σ=6.0%	μ=13.6% σ=6.3%
	θ_{error}	μ=5.12^o σ=3.62^o	μ=5.08^o σ=3.72^o
$d_{actual} >$ 4 m	d_{error}	μ=1.05m σ=0.39m	μ=1.00m σ=0.38m
	$d_{relative}$	μ=19.3% σ=6.1%	μ=18.4% σ=6.1%
	θ_{error}	μ=7.17^o σ=4.50^o	μ=7.23^o σ=4.38^o

TABLE I
Particle Filter accuracy after convergence

Results are shown in Table I split into three categories– net error for all robot to tag distances, for robot to tag distances of $d \leq$ 4m and for $d >$ 4m. The region where $d \leq$ 4m exercises the model primarily in the line-of-sight region where multipath is insignificant, while the other two categories include significant ground and ceiling-bounce multipath contributions. From additional experiments involving extended transmit power versus read distance, shown in Figure 8, we observe that the multipath models including ground and ceiling bounces are necessary to obtain good accuracy when $d >$ 4m.

VII. Conclusions

We have built and evaluated what we believe to be the first mobile robot equipped with a UHF RFID system that includes a multiple antenna UHF RFID reader as well as a particle filter implementation incorporating a multipath RF propagation model. This work presents a new particle filter framework for interpreting signals from passive UHF RFID tags that makes use of continuous-valued statistics derived from the RFID signal itself.

In our experiments the system is shown to estimate the pose of UHF RFID tags in a real-world environment without requiring *a priori* training or map-building. The system exhibits 6.1 deg. mean bearing error and 0.69m mean range error over robot to tag distances of over 4m in an environment with significant multipath. While these numbers may not seem impressive when compared to typical laser range-finder accuracy, the RFID system provides the ability to uniquely identify specific tagged locations and objects, and to discriminate among multiple tagged objects in the field at the

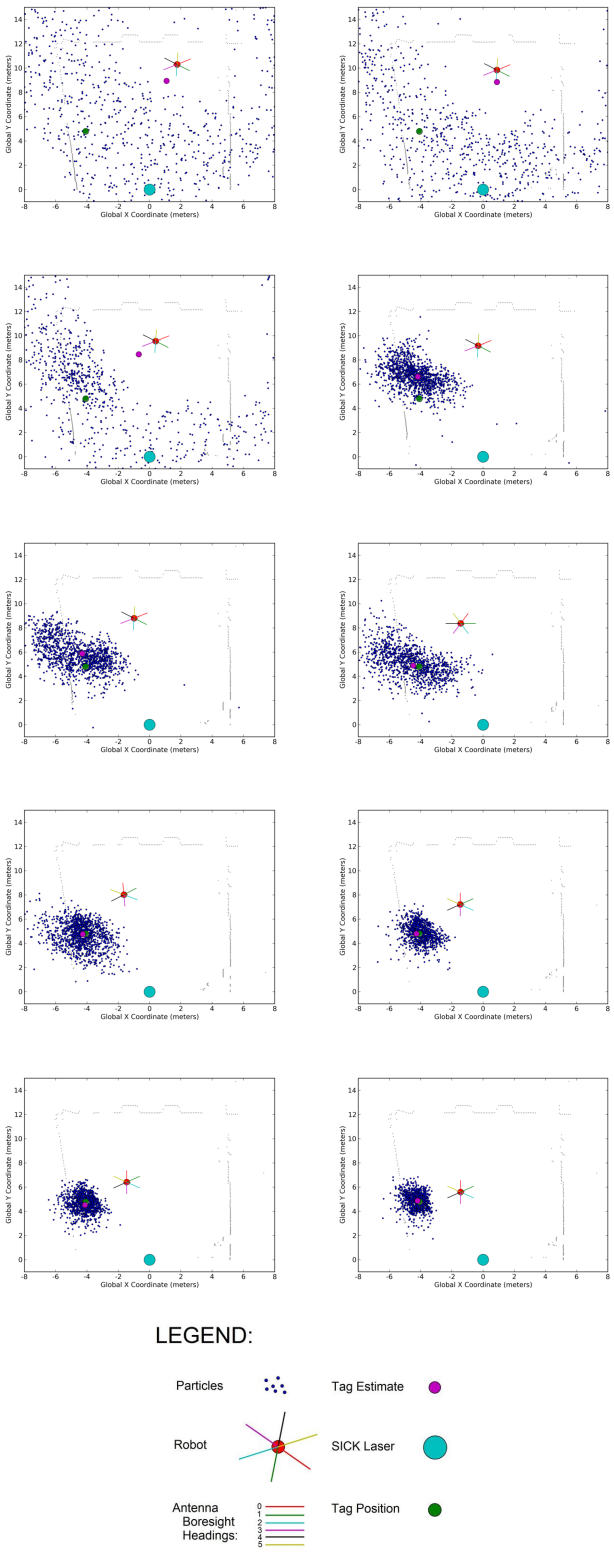

Fig. 7. Particle filter convergence. *Left-to-Right, Top-to-Bottom:* Time steps 1 through 36 in steps of 4 (≈7.2m robot travel, filter employs 1000 particles).

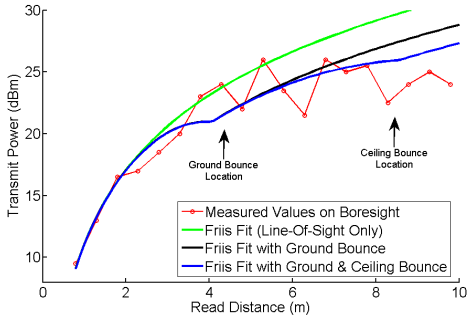

Fig. 8. Effect of multipath on Friis model estimated read distance on antenna boresight.

same time, which are important capabilities that a laser range-finder does not provide. We expect that the combination of this type of RFID range-bearing system with a laser range finder will provide especially promising results for indoor navigation and interaction with tagged objects. We thank Georgia Tech's Health Systems Institute for support through its seed grant program.

REFERENCES

[1] EPC Global US, "Class 1 Generation 2 UHF RFID protocol for operation at 860MHz-960MHz, version 1.0.9," Available online, *http://www.epcglobalus.org/*.

[2] V. Pillai, H. Heinrich, D. Dieska, P. Nikitin, R. Martinez, and K. Rao, "An ultra-low-power long range battery/passive RFID tag for UHF and microwave bands with a current consumption of 700 na at 1.5 v," *IEEE Transactions on Circuits and Systems I*, vol. 54, no. 7, pp. 1500–1512, July 2007.

[3] D. Hahnel, W. Burgard, D. Fox, K. Fishkin, and M. Philipose, "Mapping and localization with RFID technology," in *Proceedings of IEEE International Conference on Robotics and Automation*, vol. 1, 26 April-1 May 2004, pp. 1015–1020.

[4] M. Shiomi, T. Kanda, H. Ishiguro, and N. Hagita, "Interactive humanoid robots for a science museum," in *Proceedings of ACM SIGCHI/SIGART Conference on Human-Robot Interaction*. New York, NY, USA: ACM, 2006, pp. 305–312.

[5] O. Kubitz, M. Berger, M. Perlick, and R. Dumoulin, "Application of radio frequency identification devices to support navigation of autonomous mobile robots," in *Proceedings of IEEE 47th Vehicular Technology Conference*, vol. 1, 4-7 May 1997, pp. 126–130.

[6] V. Kulyukin, C. Gharpure, J. Nicholson, and S. Pavithran, "RFID in robot-assisted indoor navigation for the visually impaired," in *Proceedings of IEEE/RSJ International Conference on Intelligent Robots and Systems*, vol. 2, 28 Sept.-2 Oct. 2004, pp. 1979–1984.

[7] V. Ziparo, A. Kleiner, B. Nebel, and D. Nardi, "RFID-based exploration for large robot teams," in *Proceedings of IEEE International Conference on Robotics and Automation*, 10-14 April 2007, pp. 4606–4613.

[8] M. Kim, H. W. Kim, and N. Y. Chong, "Automated robot docking using direction sensing RFID," in *Proceedings of IEEE International Conference on Robotics and Automation*, 10-14 April 2007, pp. 4588–4593.

[9] Se–gon Roh, Y. H. Lee, and H. R. Choi, "Object recognition using 3D tag-based RFID system," in *Proceedings of IEEE/RSJ International Conference on Intelligent Robots and Systems*, Oct. 2006, pp. 5725–5730.

[10] S. Thrun, W. Burgard, and D. Fox, *Probabilistic Robotics*. MIT Press, 2005.

[11] D. M. Pozar, *Microwave Engineering*, 4th ed. Wiley and Sons, 2004, pg. 648.